



BUBBLE GROWTH IN SUPERHEATED SOLUTIONS WITH A NON-VOLATILE SOLUTE

OSAMU MIYATAKE

Department of Chemical Engineering, Kyushu University, Fukuoka 812, Japan

ITSUO TANAKA

Division of Biological Production System, Gifu University, Gifu 501-11, Japan

and

NOAM LIOR[†]

Department of Mechanical Engineering and Applied Mechanics, University of Pennsylvania, Philadelphia, PA 19104-6315, U.S.A.

(First received 30 April 1993; accepted in revised form 9 September 1993)

Abstract—Growth of single bubbles in a uniformly superheated binary solution containing a non-volatile solute was studied both experimentally, using an aqueous solution of NaCl at mass fractions of 0.05 and 0.20, an initial temperature range of 40–80°C and an applied initial superheat range of 1.7–16.5°C, and theoretically, with very good agreement between the experimental and theoretical results. The experimental technique developed, using an electrolytically nucleated bubble, was found to be excellent for single-bubble growth studies and photography. Some of the principal conclusions are that increasing the concentration of the non-volatile solute at a given initial solution temperature reduces the bubble growth rate when the far-field pressure is dropped to a fixed value. The effect of concentration on the bubble growth rate becomes smaller when the far-field pressure is reduced to bring the solution to either a fixed superheat, or to a fixed initial pressure difference between the bubble interior and exterior, leading to a conclusion that it is preferable to study and correlate bubble growth rates by using the superheat and this pressure difference as parameters.

1. INTRODUCTION

Bubble growth in a superheated liquid is a key construct of the flash evaporation process. A considerable amount of theoretical and experimental work on such bubble growth has been conducted [cf. review by Plesset and Prosperetti (1977), van Stralen and Zijl (1978) and Prosperetti (1982)], mostly considering pure liquids, and would not be summarized here. Very little is known, however, about bubble growth in superheated solutions with a non-volatile solute, a topic of both fundamental and practical importance, with applications including a wide variety of separation processes such as water desalination, and energy conversion processes such as ocean-thermal energy conversion, geothermal power generation, and nuclear reactor safety.

Amongst the small number of papers on bubble growth in superheated binary solutions, Scriven (1959) has described the general approach to modeling uniformly heated spherically symmetric bubble growth of both pure liquids and binary mixtures, and has derived approximate asymptotic solutions in the heat- and mass-transfer controlled regime, followed by studies by Skinner and Bankoff (1964), Yatabe and Westwater (1966), van Stralen (1968) and Moalem-Maron and Zijl (1978).

Summarizing the state of the art, while many basic aspects of bubble growth in superheated binary

solutions have been learned, such as the basic approach to modeling and the fact that the addition of non-volatile solutes reduces the bubble growth rate, the amount of experimental data is limited to a few solutions of volatile binary components, systematic parametric experimentation to allow the evaluation of the influence of the major process parameters has not been conducted, approximate analytical solutions have been derived for simplified problems, all but one focusing only on the heat and mass transfer controlled regime and limited by the need for empirical parameters, most thermophysical properties in the analyses were considered independent of temperature and concentration, and the specific case of a solution with a non-volatile solute, such as water and salt, has not been addressed.

The primary objective of this paper is to improve the fundamental understanding of the effects of a non-volatile solute on single-bubble growth from the time of nucleation and on, by a thorough experimental study and by analysis, and to formulate a sufficiently accurate method for prediction, taking into consideration, for example, the dependence of the thermophysical properties on temperature and concentration.

2. THE EXPERIMENTAL APPARATUS AND PROCEDURE

Bubble growth in a superheated pool of aqueous NaCl solution was observed photographically through a systematic experimental parametric study aimed at determining the influence of the major para-

[†]Author to whom correspondence should be addressed.

meters on this process. Experiments on this topic which were reported in the literature [cf. Hooper and Abdelmessih (1966), Hewitt and Parker (1968), Kosky (1968), Florschuetz *et al.* (1969), and Gopalakrishna *et al.* (1987)] typically observe bubble growth in a vessel subject to sudden decompression. In that case the pressure, and thus the superheat, changes with time, and bubbles grow at unpredictably arbitrary times and positions in the vessel. It is much easier to observe a bubble which grows at one location under conditions of constant and uniform superheat. This was accomplished in this experiment by slowly decompressing a pool of the solution in a container to the new constant pressure corresponding to the desired superheat, and then, under constant surrounding pressure conditions, generating a bubble nucleus at the tip of a cathode wire by electrolyzing the superheated solution. Unlike the situation in past experiments, the absence of other bubbles in the vessel also allows the elimination of their influence on the observed bubble, another significant advantage of this technique.

As described in Fig. 1, a degassed aqueous NaCl solution (item 5 in Fig. 1) of known concentration was contained in a cylindrical glass vessel (item 1) 50 mm in diameter and 200 mm high, which served as the bubble observation chamber. Immersed in the solution were two electrodes (item 2) made of 0.24 mm diameter copper wires which, except for their flat ends, were insulated from the solution electrically. A layer of paraffin oil (item 6) was floated on the solution surface to prevent droplets of condensate falling from the vessel top from disturbing the solution, and to prevent solution top-surface evaporation and heat losses and thus improve temperature uniformity in the solution. Analysis has shown that the paraffin oil dissolved negligibly in the aqueous NaCl solution (its solubility is $< 10^{-10}$ by mole fraction) during the experiments. The bubble observation chamber was immersed in a temperature-controlled water-bath (item 7) having two transparent sides, which was used to bring the solution to the desired

temperature. Temperature uniformities in the bath and in the chamber were monitored by thermocouple rakes (items 8 and 4, respectively), each composed of three 0.5 mm diameter sheathed Chromel–Alumel thermocouples (in item 4, spaced ~ 20 mm apart).

To prevent bubble nucleation on surface irregularities of the thermocouple rake in the bubble observation chamber, it was pulled above the surface of the solution after the temperature was recorded and found to be uniform, and the pressure in the bubble observation chamber was then reduced slowly by a gradual opening of the needle valve (item 12) connecting the chamber to a large vacuum tank (item 11) which had been maintained at a prescribed lower pressure, until the pressure in the chamber became equal to that in the vacuum tank and the solution attained the desired degree of superheat. Pressures in the vacuum tank and the chamber were measured using mercury manometers (item 13). The levels of mercury in the manometers and those of the liquid (oil and solution) in the bubble observation chamber were measured using a telescopic cathetometer.

A d.c. potential of 100–130 V for pure water and a few volts for the aqueous NaCl solutions was then switched on (by item 14) between the electrodes, electrolytically forming a hydrogen bubble at the tip of the cathode. As the bubble diameter approached its critical value, it began acting as a nucleus for a water vapor bubble. Once the vapor bubble started growing, its growth rate was much more rapid than that of the hydrogen bubble [cf. Miyatake and Tanaka (1982)].

A high-speed motion-picture camera was used to photograph the bubble growth, and a film analyzer was used to measure the bubble diameter and determine the time intervals between the measured bubble diameters. A rod of 3.00 mm diameter (item 3) was in the solution near the examined bubble to provide the scale for the diameter measurements.

To ensure that the bubble-nucleation electrode diameter did not have an effect on the results, bubble growth experiments were at first repeated with elec-

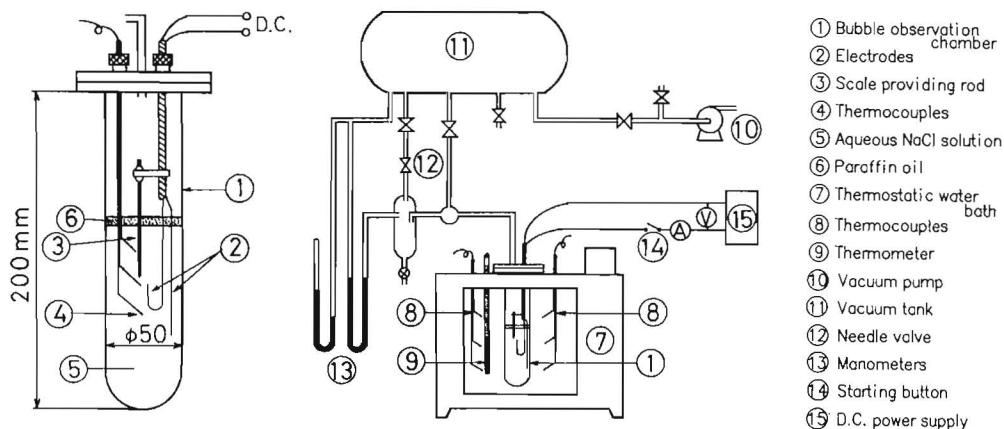


Fig. 1. The experimental apparatus.

trodes of 0.24, 0.35, and 0.67 mm diameter. The results were practically identical, and thus the 0.24 mm diameter electrode was chosen for all of the experiments reported in this paper.

The experimental errors were $\pm 0.03^\circ\text{C}$ for temperature and temperature uniformity, $\pm 2.7\text{ Pa}$ ($\pm 0.02\text{ mm Hg}$) for pressure, and $\pm 0.05\text{ ms}$ for time. While the dimensional measurement error was $\pm 0.02\text{ mm}$ for bubble size, it is noted that the bubble was typically not perfectly spherical during its growth. The asphericity of the bubble, defined by the ratio of the measured largest-to-smallest diameter for a given film frame, did not, however, exceed 1.07 up to a growth time of 10 ms. The recorded diameter was that of a perfect sphere having the same volume as the measured spheroid. The surface areas of the measured spheroid and of the sphere of equal volume, which are the dominant geometric factors in bubble growth, were found to agree within 0.12%.

Special precautions were taken to avoid the effects of contaminants on the experiment. The flash chamber was cleaned before each experiment with a medical-instruments detergent and then with distilled water. The water in the solution was prepared by ion exchange followed by distillation. The NaCl used was extra-pure chemical reagent grade. The solution was replaced with a fresh one after each bubble growth observation experiment, typically lasting not more than 30 min.

The experiments were conducted for initial solution temperatures (i.e. the temperature far from the bubble, T_∞) of 40°C and 80°C , superheats (ΔT_s) of $1.7\text{--}16.5^\circ\text{C}$ (depending on T_∞), and for NaCl (solute) mass fractions (ω_∞) of 0.05 and 0.20.

To determine the value of ΔT_s , the static pressure at the cathode-tip level was calculated as the sum of the vapor pressure above the liquid, and the static pressure rises due to the paraffin oil layer and the solution layer between the oil-solution interface and the cathode tip.

3. EXPERIMENTAL RESULTS

Figures 2(a) and (b) show the growth of a bubble for initial solution temperatures of $T_\infty = 40$ and 80°C , respectively. The time elapsed between the consecutive eight-frame columns in Fig. 2(a) is 2.15 ms and in Fig. 2(b) 1.82 ms. The bubble growth is seen to resemble very closely that of a stationary sphere: indeed, past studies (Pinto and Davis, 1971; Gopalakrishna and Lior, 1992) show that the rise of such bubbles over a period of 10 ms is smaller than 1 mm and, as mentioned in Section 2, the asphericity was < 1.07 .

In an attempt to understand the importance of the parameters associated with the observed bubble growth phenomena, and to discover the parameters which may lead to better correlation of the results or normalization of the variables, the effects of the far-field solute mass fraction (ω_∞) and solution temperature (T_∞) on the bubble growth history are presented in Figs 3–5 for different fixed values of the

far-field pressure (p_∞), superheat (ΔT_s), and of the initial pressure difference between the bubble interior and exterior (ΔP_0), respectively. The symbols in the figures indicate the experimental observations and the solid lines indicate our numerical solutions (described in Sections 4–6) for the same experimental conditions.

The observed behavior agrees with the established knowledge of bubble growth in pure liquids [cf. Plesset and Prosperetti (1977)]: after an initial brief period during which the bubble grew to a size at which the effect of bubble wall surface tension became negligible, bubble growth is dominated by inertial forces driven primarily by the pressure difference $p_v - p_\infty$ between the bubble interior and exterior, which is also almost equal to ΔP_0 because the decrease of bubble wall temperature is still comparatively small, and in that regime the growth history is linear, $R \propto t$. After some period of further growth, evaporation at the bubble wall causes the temperature there (T_i) to drop below the surrounding liquid temperature (T_∞) to a level high enough for heat transfer to the evaporating bubble-liquid interface to start dominating growth due to the consequent addition of vapor to the bubble. This changes the bubble growth relationship to $R \propto t^{1/2}$, i.e. to a non-linear one. Figures 3–5 show that the transition from the linear (inertia-controlled) regime to the non-linear (heat-transfer-controlled) one, whose rate is proportional to the rate of the reduction in T_i , occurs sooner for larger T_∞ , and for smaller ΔT_s (also see Fig. 10). It is, for example, evident from these figures that when $T_\infty = 80^\circ\text{C}$ the bubble is brought much more rapidly into the heat-transfer-controlled regime characterized by the $R \propto t^{1/2}$ shape, while at $T_\infty = 40^\circ\text{C}$ the bubble remains in the linear, inertia-controlled regime throughout the investigated period.

The observed reduction of the bubble growth rates with increasing concentration for fixed values of p_∞ (Fig. 3) is due to the consequent boiling-point elevation, i.e. the reduction of the vapor pressure inside the bubble. The effect of the concentration is seen to be much larger for higher p_∞ because the difference between the magnitudes of the bubble growth driving forces ($p_v - p_\infty$) dominating the inertia-controlled regime, and the difference between the magnitudes of the bubble growth driving forces ($T_\infty - T_i$) representing the actual driving force ($\partial T/\partial r$), dominating the heat-transfer regime, for two given concentrations, are then larger at a given T_∞ . It is interesting to note that the effect of concentration is seen to be considerable when p_∞ is the parameter held constant (Fig. 3), but that it becomes very small when ΔT_s is the parameter held constant, especially in the heat-transfer-controlled bubble growth regime (i.e. at $T_\infty = 80^\circ\text{C}$, Fig. 4), or when ΔP_0 is held constant, especially in the inertia-controlled regime (i.e. at $T_\infty = 40^\circ\text{C}$, Fig. 5). This observation is shown to be consistent with the theory, by examining the bubble growth driving force ($p_v - p_\infty$) dominating the inertia-controlled regime, and the driving force ($T_\infty - T_i$) dominating the heat-transfer-controlled regime, as

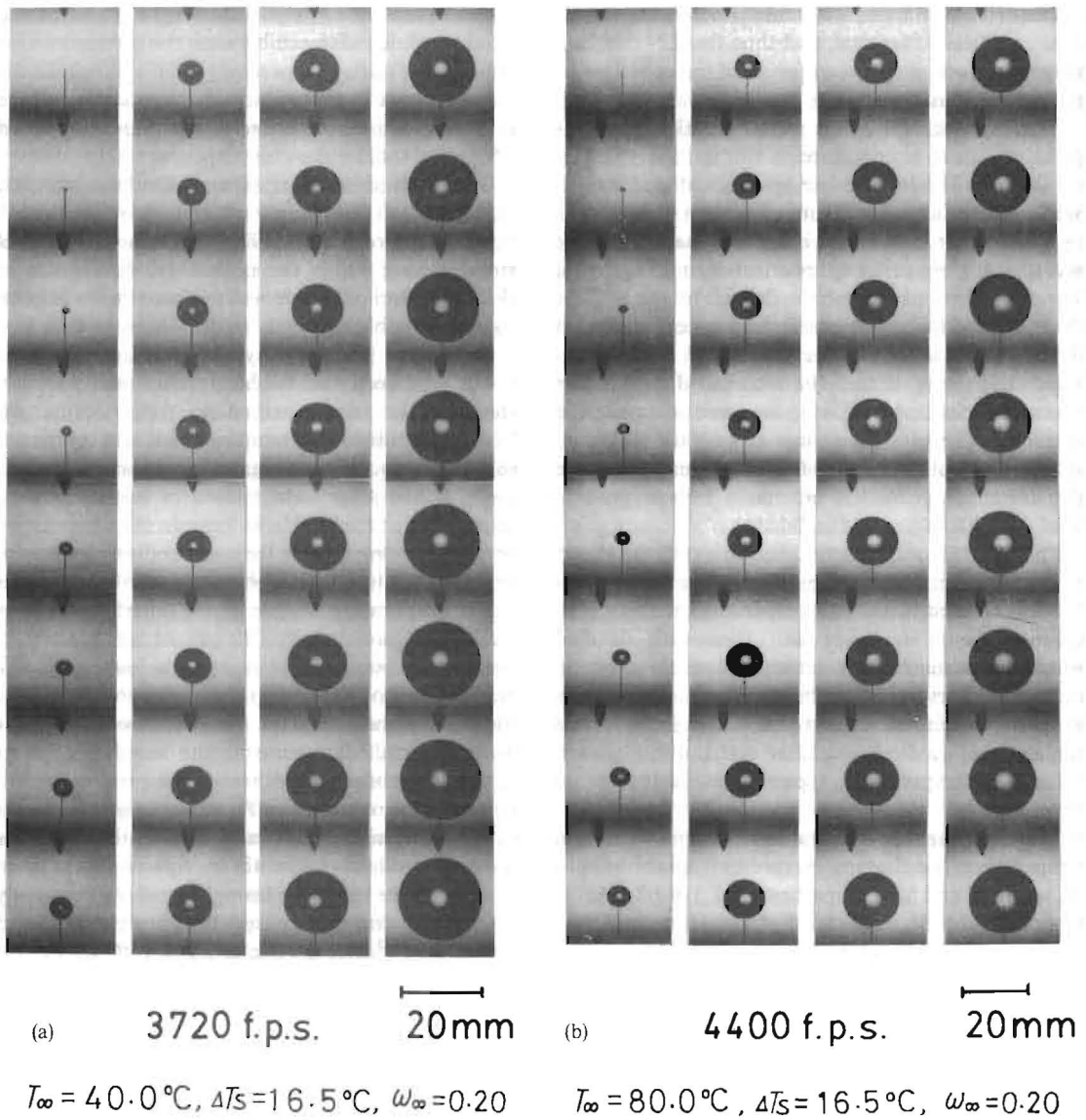


Fig. 2. Bubble growth as observed by high-speed photography (the time-sequence is from top to bottom in each column, columns arranged from left to right).

follows. When p_∞ is fixed (at constant T_∞) both driving forces increase when ω_∞ is lower, the first one due to an increase in p_v and the second due to a decrease in the saturation temperature (which is also the temperature T_i). If $\Delta T_s = T_\infty - T_e$ is fixed, p_∞ is defined at the equilibrium temperature T_e and thus both p_∞ and p_v are inversely proportional to ω_∞ . The dominant bubble growth driving force ($p_v - p_\infty$) in the inertia-controlled regime consequently becomes almost constant, affected only by the relatively weak dependence of $p_v(T)$ on concentration for the conditions examined in this study. The dominant driving force ($T_\infty - T_i$) in the heat-transfer-controlled regime also remains almost constant because T_i can vary only within the fixed range from T_∞ to T_e , and consequently the effect of ω_∞ becomes practically negligible for a specified

ΔT_s in the heat-transfer-controlled regime as seen in Fig. 4 at $T_\infty = 80^\circ\text{C}$. If ΔP_0 is specified, ω_∞ has, by definition, no effect on bubble growth in the inertia-controlled regime, as seen in Fig. 5 at 40°C .

One of the conclusions from this weak dependence of bubble growth history and rates on concentration for given ΔT_s is that experimental results relating the degree of approach to equilibrium in flash evaporation of fresh water [cf. Miyatake *et al.* (1977), Lior and Greif (1980), Miyatake *et al.* (1985), Gopalakrishna *et al.* (1987) and Miyatake *et al.* (1992, 1993)] will also be valid for moderate-concentration brines and seawater ($\omega_\infty \approx 0.07$ in commercial multi-stage flash evaporators for water desalination). It also may extend the validity of empirical correlations obtained for the approach to equilibrium in flashing of

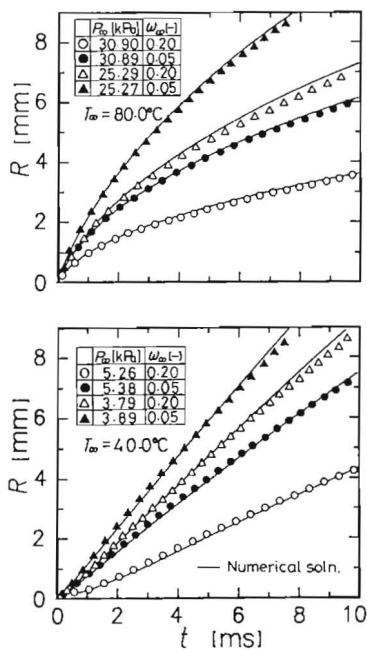


Fig. 3. The experimentally observed bubble growth history (the solid curves are our numerical solution) for different fixed values of the far-field pressure (p_∞), at two values of the solute mass fraction (ω_∞) and solution temperature (T_∞).

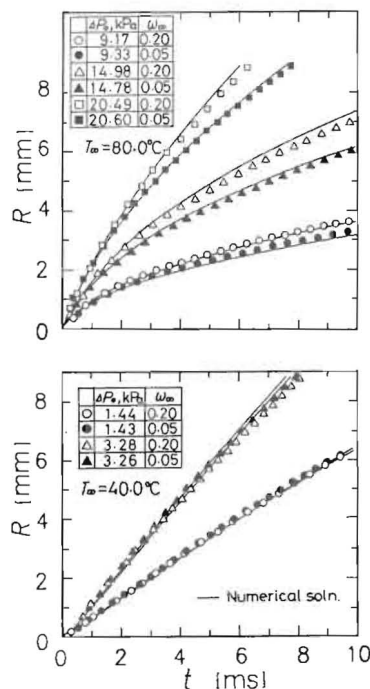


Fig. 5. The experimentally observed bubble growth history (the solid curves are our numerical solution) for different fixed values of the initial pressure difference between the bubble interior and exterior (ΔP_0), at two values of the solute mass fraction (ω_∞) and solution temperature (T_∞).

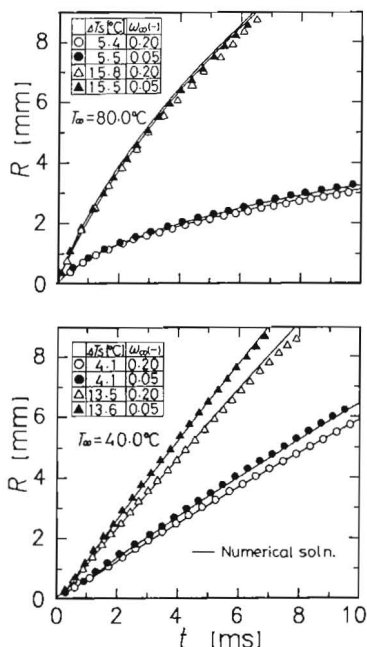


Fig. 4. The experimentally observed bubble growth history (the solid curves are our numerical solution) for different fixed values of the superheat (ΔT_s), at two values of the solute mass fraction (ω_∞) and solution temperature (T_∞).

saline water at specific concentrations [cf. Lior (1986)] to a wider range of concentrations.

Figure 6 shows the bubble radius history with more values of the superheat as the parameter. It can again

be seen that bubble growth is inertia-controlled ($R \propto t$) at the lower solution temperatures and higher superheats, and that it is heat-transfer-controlled at the higher solution temperatures and lower superheats. The characteristic occurrence of a short delay in bubble growth due to the strong effect of bubble wall surface tension when the solution temperature and superheat are low is also evident (it can also be seen in Fig. 3).

4. ANALYTICAL MODELING

Guided by the experimental results and conclusions, a theoretical model was developed to predict transient bubble growth in superheated solutions with a non-volatile solute, which could be validated by the experimental results obtained. As commonly done [cf. Scriven (1959), Mikić *et al.* (1970) and Theofanous and Patel (1976)] and also confirmed by our and other [cf. Dergarabedian (1953) and Hooper and Abdelmessih (1966)] experiments, it was assumed in the analysis that the bubble shape is spherical. Derived from the equations of continuity and motion, the equation for the transient bubble radius is [cf. Scriven (1959)]

$$R(t) \frac{d^2 R(t)}{dt^2} + \frac{3}{2} \left[\frac{dR(t)}{dt} \right]^2 = \frac{1}{\rho_l} \left\{ \left[p_v(t) - \frac{2\sigma}{R(t)} - \frac{4\mu_l}{R(t)} \frac{dR(t)}{dt} \right] - p_\infty \right\} \quad (1)$$

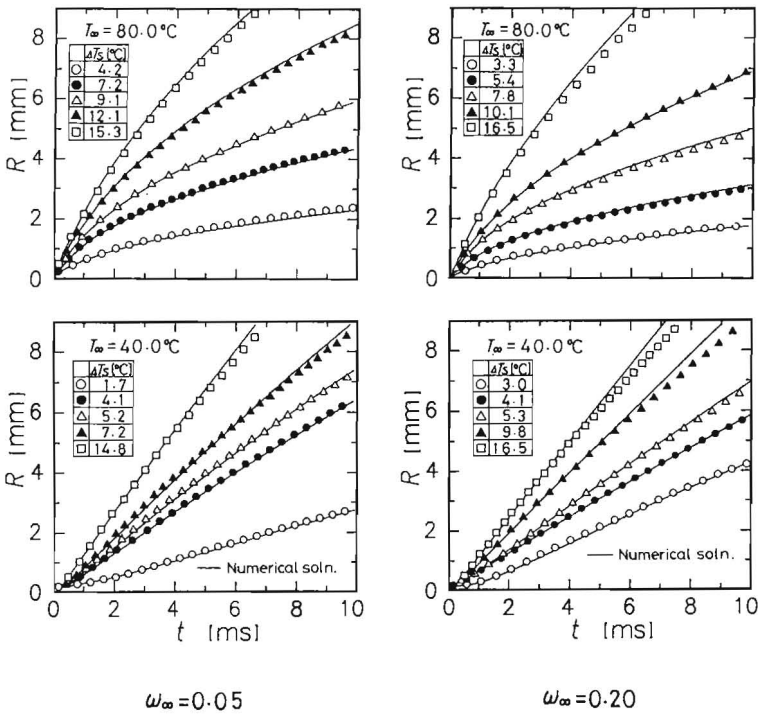


Fig. 6. The experimentally observed bubble growth history (the solid curves are our numerical solution) for various values of the superheat (ΔT_s), at two values of the solute mass fraction (ω_∞) and solution temperature (T_∞).

where p_v is the vapor pressure in the bubble, p_∞ the pressure in the solution far from the bubble, ρ_l the solution density, μ_l the dynamic viscosity of the solution, and σ the surface tension on the bubble wall.

Using the expression $\delta_i/R \leq Ja^{-1}$, which relates the thermal boundary layer thickness δ_i -bubble radius R ratio with the Jakob number Ja (Prosperetti and Plesset, 1978), Miyatake and Tanaka (1982) have shown that for $Ja > 10$ the radius growth-rate results obtained by using the thin boundary layer assumption are indistinguishable from those obtained by Dalle Donne and Ferranti (1975) for sodium at $Ja = 2.98$ –566, and by Saito and Shima (1977) for water at $Ja = 1070$, from the numerical solution of the full bubble growth problem. Since the numerical study performed here was in the range of $Ja > 36$, the thin boundary layer approximation is valid and thus the thin boundary layer analytical solution of the energy and continuity equations obtained by Plesset and Zwick (1952, 1954) for the temperature T_i of the solution at the bubble wall (recalling that subscript i denotes the bubble wall, i.e. the vapor-liquid interface), shown in eqs (2) and (3) below, was used:

$$T_i(t) = T_\infty - \left(\frac{\alpha_l}{\pi}\right)^{1/2} \int_0^t F(t, x) \left[\frac{\partial T(r, x)}{\partial r}\right]_i dx \quad (2)$$

where T_∞ is the temperature of the solution far from the bubble, α_l the thermal diffusivity of the solution, and $F(t, x)$ the function

$$F(t, x) = R^2(x) \left[\int_x^t R^4(y) dy \right]^{-1/2} \quad (3)$$

Due to the similarity between the equations of energy and mass transfer (for constant density of the solution), and because the concentration boundary layer is even thinner than the thermal boundary layer, one can derive from eqs (2) and (3) an expression for the mass fraction of the solute at the bubble wall by replacing the solution temperature T with the solute mass fraction ω , and the solution thermal diffusivity α_l with the solute mass diffusivity D , resulting in

$$\omega_i(t) = \omega_\infty - \left(\frac{D}{\pi}\right)^{1/2} \int_0^t F(t, x) \left[\frac{\partial \omega(r, x)}{\partial r}\right]_i dx \quad (4)$$

where ω_∞ is the mass fraction of the solute in the solution far from the bubble and $F(t, x)$ was defined by eq. (3).

The temperature and concentration gradients at the bubble interface can be obtained from heat and mass balances at that location, respectively:

$$4\pi R^2(t)k_l \left[\frac{\partial T(r, t)}{\partial r}\right]_i = h_{fg}W_v(t) \quad (5)$$

$$-4\pi R^2(t)\rho_l D \left[\frac{\partial \omega(r, t)}{\partial r}\right]_i = \left[\frac{\omega_i(t)}{1 - \omega_i(t)}\right] W_v(t) \quad (6)$$

where k_l is the thermal conductivity of the solution, h_{fg} the latent heat of vaporization, and W_v the mass rate of evaporation expressed as

$$W_v(t) = \frac{d[(4/3)\pi\rho_v(t)R^3(t)]}{dt} \quad (7)$$

The density ρ_v of the generated vapor, which is super-

heated due to the boiling point elevation ($T_i - T_s$), can be expressed as

$$\rho_v(t) = \frac{273.15 + T_s(t)}{273.15 + T_i(t)} (\rho_{v,s})_{T_s} \quad (8)$$

where $(\rho_{v,s})_{T_s}$ is the saturation density of vapor, evaluated at the saturation temperature T_s of the pure solvent.

The saturation temperature T_s of the pure solvent, which is needed for evaluating p_v in eq. (1) and ρ_v in eq. (8), was determined from the relation

$$p_v(t) = P_{T_s}^* = P_{T_s, \omega_i} \quad (9)$$

where P^* and P are the vapor pressures of pure solvent and solution, respectively.

A bubble which has the critical radius R_c is in unstable equilibrium. An infinitesimal increase, δ , in the bubble radius will thus initiate growth, hence defining the initial bubble radius, $R(0)$, as

$$R(0) = R_c(1 + \delta) = \frac{2\sigma(1 + \delta)}{\Delta P_0} \quad (10)$$

where we recall that ΔP_0 is the initial pressure difference between the bubble interior and exterior defined by

$$\Delta P_0 = p_v(0) - p_\infty = P_{T_s, \omega_\infty} - p_\infty \quad (11)$$

The superheat of the solution, ΔT_s , is defined by

$$\Delta T_s = T_\infty - T_e \quad (12)$$

using the equilibrium temperature T_e which satisfies the relation

$$p_\infty = P_{T_e, \omega_\infty} \quad (13)$$

i.e. the temperature at which the solution of concentration ω_∞ has the same vapor pressure as the pressure p_∞ in the solution far from the bubble.

Given T_∞ , the solution temperature far from the bubble (i.e. the initial uniform temperature of the solution), and p_∞ , the pressure in the solution, or, alternatively, given the superheat ΔT_s or the pressure difference ΔP_0 , evaluated from eqs (12) and (13), or eq. (11), respectively, the relationship between the bubble radius R and the time t can be determined by solving the simultaneous system of equations (1)–(9) subject to the initial conditions composed of eq. (10) and

$$\left[\frac{dR(t)}{dt} \right]_{t=0} = \left[\frac{d^2R(t)}{dt^2} \right]_{t=0} = 0 \quad (14)$$

[the second initial condition above needs to be specified for the finite difference scheme because in eq. (10) $\delta \neq 0$].

5. THE NUMERICAL SOLUTION PROCEDURE

A finite difference forward-matching implicit method was used to solve the above system of equations iteratively at each time step. The solution was iterated at a given time step until the change in the moduli of R and ρ_v , $(|R^{(m)} - R^{(m-1)}|/R^{(m-1)})$ and $(|\rho_v^{(m)} - \rho_v^{(m-1)}|/\rho_v^{(m-1)})$, respectively, where m is the

iteration number index at a given time step) became $< 10^{-5}$, and t was then increased to the new time step. A variable time-step grid was employed, fine at the beginning and gradually coarser as time increased, by having 91 time steps for each ten-fold increase in t . Totally a minimum of 370 time steps were used in the range $t = 0-10^{-2}$ s.

As stated above, T_∞ and p_∞ , or ΔT_s or ΔP_0 were given for each computational run, and a value of $\delta = 10^{-4}$ was chosen for use in eq. (10), since it was found that a deviation of this magnitude in the initial bubble radius had an insignificant effect on the numerical results.

All properties used in the analytical modeling were temperature and concentration-dependent, calculated by empirical formulas either given in the literature or developed by the authors from available experimental data. The properties and sources for the correlations are vapor pressure (Fabuss and Korosi, 1966; JSME, 1971), mass diffusivity [using the relationship of Olson and Walton (1951) to correlate the experimental data of NRC (1929), Stokes (1950), Fell and Hutchinson, (1971) and Chang and Myerson, (1985)], viscosity (JSME, 1962; ORNL, 1966), thermal conductivity (Yusufova *et al.*, 1978; Ozbek and Phillips, 1980), specific heat (NRC, 1927, 1929; Yusufova *et al.*, 1978), vapor density (Sato, 1974), solution density (NRC, 1928a; JSSWS, 1974), latent heat of evaporation (JSME, 1980), and surface tension (NRC, 1928b; Yusufova *et al.*, 1978; JSME, 1980). The properties σ and h_{fg} , which are used at the bubble interface, were evaluated at temperature T_i and concentration ω_i . All the other physical properties, which were not indexed above by a temperature and concentration, were evaluated at temperature $(T_i + T_\infty)/2$ and concentration $(\omega_i + \omega_\infty)/2$.

6. THE NUMERICAL SOLUTION RESULTS AND COMPARISON WITH EXPERIMENTS

Figures 3–6 in Section 3, which present the experimental results, also present the comparison of the experimental results with the numerically obtained results shown by solid lines. The agreement between the experimental and numerical results is seen to be very good in all the bubble growth regimes, beginning with the surface-tension-induced initial delay at low radii and solution temperatures and superheats, through the linear ($R \propto t$) inertia-controlled regime at lower solution temperatures, and into the heat-transfer-controlled regime occurring at higher solution temperatures and characterized by $R \propto t^{1/2}$.

Figure 7 shows the computed bubble radius histories under two fixed values of the far-field pressure p_∞ which correspond to $\Delta T_s = 5$ and 20°C for pure solvent (water) of a given temperature T_∞ , and for solute mass fractions ω_∞ of 0, 0.05, 0.10 and 0.20; Figs 8 and 9 show the computed bubble radius histories for fixed values of the superheat ΔT_s , and for fixed values of the initial pressure difference ΔP_0 between the bubble interior and exterior, respectively, at

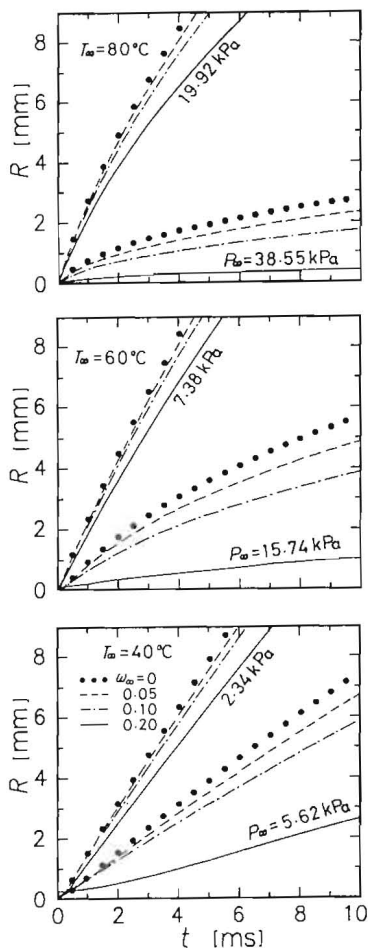


Fig. 7. The computed bubble growth histories at four solute mass fractions ω_∞ , for two fixed values of the far-field pressure p_∞ which correspond to $\Delta T_s = 5^\circ\text{C}$ and 20°C for pure solvent (water) at three given temperatures T_∞ .

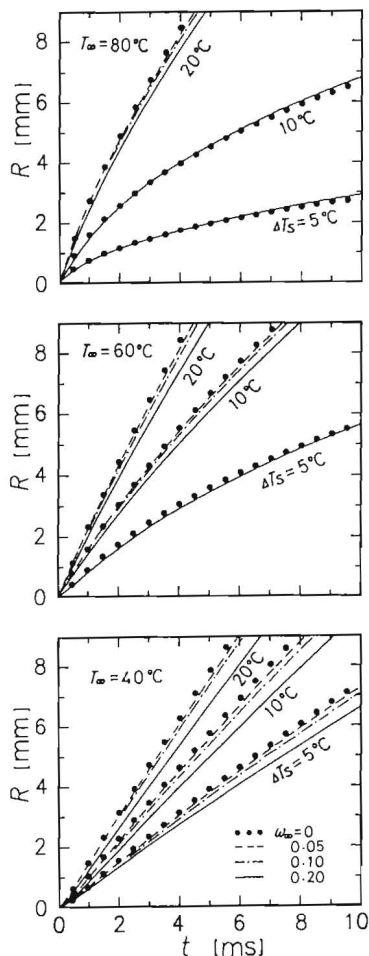


Fig. 8. The computed bubble growth histories at four solute mass fractions (ω_∞), for three fixed values of the superheat (ΔT_s), at three given solution temperatures (T_∞).

the same given concentrations ω_∞ and temperatures T_∞ . The conclusions are the same as those discussed in Section 3 for the experimental results in Figs 3–5; Figs 7–9 provide more detail.

Figure 10 shows the history of the bubble wall temperature T_i [in terms of the non-equilibrium fraction $(T_i - T_e)/(T_\infty - T_e)$] and the bubble wall solute mass fraction ω_i (in terms of $\omega_i - \omega_\infty$) for fixed values of the superheat ΔT_s . It is seen that the rate of descent of T_i towards T_e increases as T_∞ increases and as ΔT_s and ω_∞ decrease, while the rate of ascent of ω_i from its lowest value of ω_∞ is proportional to the magnitudes of T_∞ , ΔT_s , and ω_∞ .

Comparison of these results with Fig. 8 shows that the slow rate of descent of T_i , caused by low T_∞ and high ΔT_s , thus occurs in the inertia-controlled regime, in which thus the bubble stays longer because this slow rate of descent of T_i also produces a relatively low heat-transfer driving force. This also explains the fact that the concentration (ω_∞) has the largest effect at these conditions (Fig. 8): in the inertia-controlled regime, where bubble growth is driven primarily by

$(p_v - p_\infty)$, the vapor pressure (p_v) is directly related to the concentration. Accordingly, when ΔP_0 is taken as a parameter, ω_∞ has little effect on the bubble growth in this regime.

As stated in Section 4, this analysis took carefully into consideration the effects of temperature and concentration on the thermophysical properties of the solution and the vapor. It is interesting to examine the effect of these properties' variation on the results. Figure 11 shows the effects of the solute concentration at the bubble wall and of the superheat of the generated vapor due to the boiling point elevation on bubble growth solutions at different values of T_∞ and ΔT_s . The solid lines represent the solutions under physically correct assumptions for the bubble wall concentration and vapor density, $\omega_i = \omega_i$ and $\rho_v = \rho_v$, meaning that these variables take the correct values at the interface, as determined by the set of equations given in Section 4, and by the property correlations used.

Assuming that the concentration at the bubble wall does not change during evaporation and remains con-

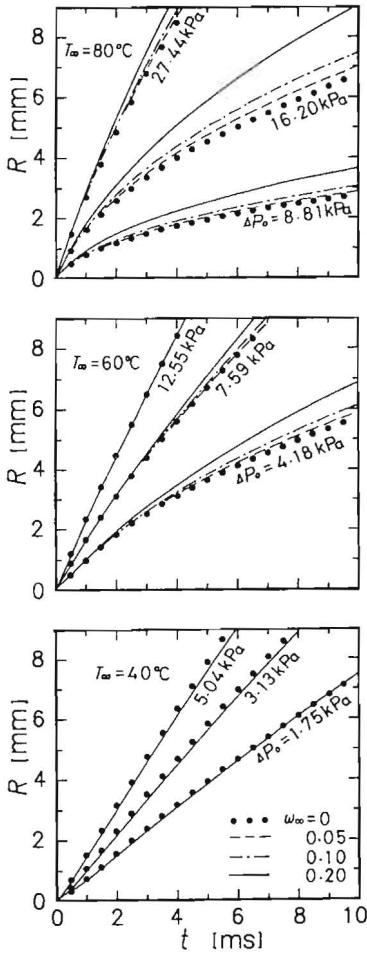


Fig. 9. The computed bubble growth histories at four solute mass fractions (ω_∞), for three fixed values of the initial pressure difference between the bubble interior and exterior (ΔP_0), at three given solution temperatures (T_∞).

stant at ω_∞ , i.e. $\omega_i = \omega_\infty$, $\rho_v = \rho_v$ (the solid symbols in Fig. 11), results in a solution indicating bubble growth rates which are somewhat (8.3% at $T_\infty = 80^\circ\text{C}$) higher than the correct ones, primarily because in reality $\omega_\infty < \omega_i$ and therefore the vapor pressure in the bubble is lower due to its inverse proportionality to the concentration. In the third assumption, $\omega_i = \omega_i$, $\rho_v = (\rho_{v,s})_{T_i}$, the vapor density at the bubble wall is assumed to correspond to that at the saturation conditions for T_i , ignoring the fact that the generated vapor is actually superheated. As shown by the empty symbols in Fig. 11, this assumption results in solutions indicating that the bubble growth rate is lower (by 17.8% at $T_\infty = 80^\circ\text{C}$) than the correct one, obviously because the generated vapor density is higher when the superheat is ignored. It can also be seen from Fig. 11 that the effects of the simplifying assumptions $\omega_i = \omega_\infty$ and $\rho_v = (\rho_{v,s})_{T_i}$ are practically negligible (3.5% at $T_\infty = 80^\circ\text{C}$) when the concentration is low ($\omega_\infty = 0.05$), but become significant (17.8% at $T_\infty = 80^\circ\text{C}$) when the concentration is high

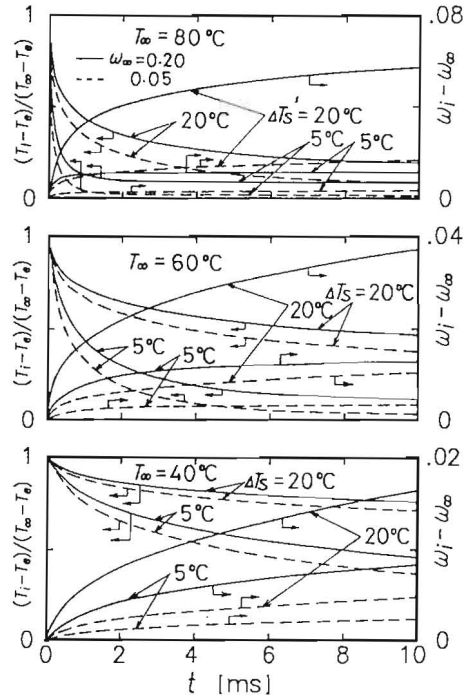


Fig. 10. The histories of the non-equilibrium fraction $[(T_i - T_e)/(T_\infty - T_e)]$ and of the change of the bubble wall solute mass fraction ($\omega_i - \omega_\infty$) for two values of the solute mass fractions (ω_∞) and the superheat (ΔT_s), at three given solution temperatures (T_∞).

($\omega_\infty = 0.20$), phenomena consistent with the above reasoning. It is also seen that the effect of the assumptions $\omega_i = \omega_i$, $\rho_v = (\rho_{v,s})_{T_i}$ are small (4.9% at $T_\infty = 40^\circ\text{C}$) in the inertia-controlled bubble growth region since bubble growth in that region is primarily driven by the pressure difference between the bubble interior and exterior and is almost independent of ρ_v .

7. CONCLUSIONS

Growth of single bubbles in a uniformly superheated binary solution containing a non-volatile solute was studied both experimentally (using an aqueous solution of NaCl) and theoretically, with very good agreement between the experimental and theoretical results. The experimental technique developed, using an electrolytically nucleated bubble, is new, allowing the observation of single-bubble growth at a fixed location. The principal conclusions are as follows:

(a) The experimental technique developed was found to be excellent for single-bubble growth studies and photography.

(b) When compared with bubble growth in pure liquids, the non-volatile solute reduces the vapor pressure of the solution (elevates the boiling point), which is also the vapor pressure in the bubble, and thus reduces the bubble growth rate. As expected, this reduction in growth rate increases with the solution concentration.

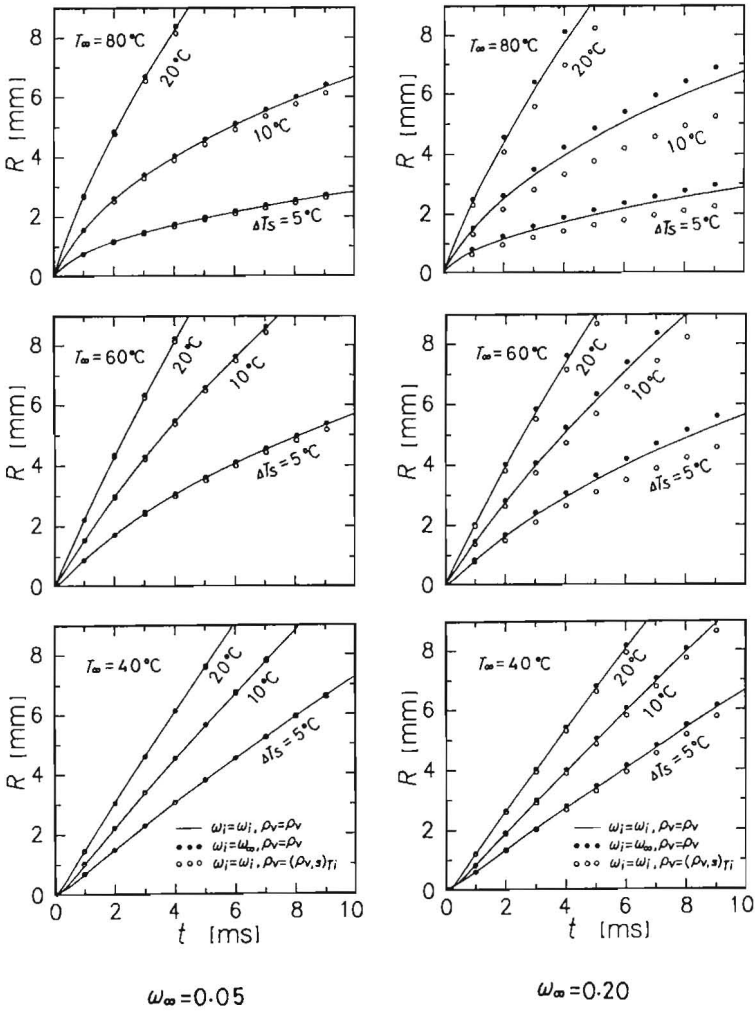


Fig. 11. Comparison of the effects of the solute concentration at the bubble wall and the superheat of the generated vapor due to the boiling point elevation on bubble growth solutions at different values of T_∞ and ΔT_s . The solid lines represent the solutions under physically correct assumptions for the bubble wall concentration and density, $\omega_i = \omega_i$ and $\rho_v = \rho_v$. $\omega_i = \omega_\infty$, $\rho_v = \rho_v$ (●) corresponds to the simplifying assumption that the concentration at the bubble wall does not change during evaporation and remains constant at ω_∞ ; $\omega_i = \omega_i$, $\rho_v = (\rho_v, s)_{T_i}$ (○) corresponds to the simplifying assumption that the vapor density at the bubble wall is that at the saturation conditions for T_i .

(c) This effect of concentration is quite significant when the solution, initially at equilibrium at a prescribed temperature, is brought to the superheated state by reducing the far-field (or ambient) pressure to a fixed value. The effect of concentration is much smaller, however, when the far-field pressure is reduced to bring the solution to either a fixed superheat, especially in the heat-transfer-controlled bubble growth regime, or to a fixed initial pressure difference between the bubble interior and exterior, especially in the inertia-controlled regime.

(d) The weak dependence of bubble growth rate on concentration for fixed superheat and fixed initial pressure difference between the bubble interior and exterior, described in conclusion (c), leads to the conclusion that it is preferable to study and correlate

bubble growth rates by using the superheat and this pressure difference as parameters (rather than using the far-field pressure) in each regime.

(e) Ignoring the effects of the solute concentration at the bubble wall and of the superheat of the generated vapor on bubble growth in the theoretical solution introduces negligible errors at the lower concentrations and solution temperatures considered, but these errors increase with concentration and temperature. The latter effect is specially evident in the heat-transfer-controlled bubble growth regime, the error becoming as high as 18% at the highest concentrations and temperatures considered in this study.

(f) The weak dependence of bubble growth history and rates on concentration for a given ΔT_s , discovered

in this study indicates that experimental results and correlations relating the degree of approach to equilibrium in flash evaporation of fresh water are also valid for moderate-concentration brines and seawater, and those obtained for saline water at specific concentrations would be applicable to a wider range of concentrations.

NOTATION

c_l	specific heat of solution, J/kg K
D	mass diffusivity, m^2/s
h_{fg}	latent heat of vaporization, J/kg
Ja	Jakob number ($= \rho_l c_l \Delta T_s / \rho_v h_{fg}$), dimensionless
k_l	thermal conductivity of solution, W/m K
p_v	pressure of vapor in bubble, Pa
p_x	pressure in solution far from bubble, Pa, kPa in the figures
P	vapor pressure of solution, Pa
P^*	vapor pressure of pure solvent, Pa
r	radial coordinate measured from bubble center, m
R	bubble radius, m
R_c	critical bubble radius ($= 2\sigma/\Delta P_0$), m
t	time, s, ms in the figures
T	temperature of solution, $^{\circ}C$
T_e	equilibrium temperature of solution corresponding to p_{∞} , $^{\circ}C$
T_s	saturation temperature of pure solvent corresponding to p_{∞} , $^{\circ}C$
W_v	mass rate of evaporation, kg/s
<i>Greek letters</i>	
α_l	thermal diffusivity of solution, m^2/s
δ	infinitesimal deviation, dimensionless
δ_l	thermal boundary layer thickness in solution, m
ΔP_0	initial pressure difference between the bubble interior and exterior [$= p_v(0) - p_{\infty}$], Pa
ΔT_s	superheat ($= T_{\infty} - T_e$), $^{\circ}C$
μ_l	viscosity of solution, Pa s
ρ_l	density of solution, kg/m^3
ρ_v	density of generated vapor, kg/m^3
$\rho_{v,s}$	saturation density of vapor, kg/m^3
σ	surface tension at the bubble wall, N/m
ω	mass fraction of solute in solution, dimensionless

Subscripts

i	value at the bubble wall
∞	value far from the bubble

REFERENCES

- Chang, Y. C. and Myerson, A. S., 1985, The diffusivity of KCl and NaCl in concentrated, saturated, and superheated aqueous solutions. *A.I.Ch.E. J.* **31**, 890–894.
- Dalle Donne, M. and Ferranti, M. P., 1975, The growth of vapor bubbles in superheated sodium. *Int. J. Heat Mass Transfer* **18**, 477–493.
- Dergarabedian, P., 1953, The rate of growth of vapor bubbles in superheated water. *J. appl. Mech.* **20**, 537–545.
- Fabuss, B. M. and Korosi, A., 1966, Vapour pressures of binary aqueous solutions of NaCl, KCl, Na_2SO_4 and $MgSO_4$ at concentrations and temperatures of interest in desalination processes. *Desalination* **1**, 139–148.
- Fell, C. J. D. and Hutchison, H. P., 1971, Diffusion coefficients for NaCl and KCl in water at elevated temperatures. *J. chem. Engng Data* **16**, 427–429.
- Florschuetz, L. W., Henry, C. L. and Rashid Khan, A., 1969, Growth rates of free vapor bubbles in liquid at uniform superheats under normal and zero gravity conditions, *Int. J. Heat Mass Transfer* **12**, 1465–1489.
- Gopalakrishna, S. and Lior, N., 1990, Bubble growth in flash evaporation, in *Proceedings of the 9th International Heat Transfer Conference*. Jerusalem, Israel, Vol. 3, pp. 73–78. Hemisphere, New York.
- Gopalakrishna, S. and Lior, N., 1992, Analysis of bubble translation during transient flash evaporation. *Int. J. Heat Mass Transfer* **35**, 1753–1761.
- Gopalakrishna, S., Purushothaman, V. and Lior, N., 1987, An experimental study of flash evaporation from liquid pools. *Desalination* **65**, 139–151.
- Hewitt, H. C. and Parker, J. D., 1968, Bubble growth and collapse in liquid nitrogen. *Trans. ASME Ser. C* **90**, 22–26.
- Hooper, F. C. and Abdelmessih, A. H., 1966, The flashing of liquid at higher superheats, in *Proceedings of the 3rd International Heat Transfer Conference*, Chicago, pp. 44–50.
- JSME, 1962, *Dennetsu Kogaku Shiryo (Materials of Heat Transfer Engineering)*, p. 215. Japan Society of Mechanical Engineers, Tokyo.
- JSME, 1971, *Jokihyo Senzu (Steam Tables and Charts)*, p. 1. Japan Society of Mechanical Engineers, Tokyo.
- JSME, 1980, *Steam Tables*, pp. 10 and 123. Japan Society of Mechanical Engineers, Tokyo.
- JSSWS, 1974, *Kaisui Riyo Handbook (Handbook of Seawater)*, p. 111 and 123. Japan Society of Sea Water Science, Tokyo.
- Kosky, P. G., 1968, Bubble growth measurement in uniformly superheated liquids. *Chem. Engng Sci.* **23**, 695–706.
- Lior, N., 1986, Formulas for calculating the approach to equilibrium in open channel flash evaporators for saline water. *Desalination* **60**, 223–249.
- Lior, N. and Greif, R., 1980, Some basic observations on heat transfer and evaporation in the horizontal flash evaporator. *Desalination* **33**, 269–286.
- Mikić, B. B., Rohsenow, W. H. and Griffith, P., 1970, On bubble growth rates. *Int. J. Heat Mass Transfer* **13**, 657–666.
- Miyatake, O. and Tanaka, I., 1982, Bubble growth in uniformly superheated water at reduced pressures, 1st Report, 2nd Report. *Trans. JSME, Ser. B* **48**, 355–363, 364–371.
- Miyatake, O., Fujii, T. and Hashimoto, T., 1977, An experimental study of multi-stage flash evaporation phenomena. *Heat Transfer Japanese Res.* **6**(6), 25–35.
- Miyatake, O., Hashimoto, T. and Lior, N., 1992, The liquid flow in multi-stage flash evaporators. *Int. J. Heat Mass Transfer* **35**, 3245–3257.
- Miyatake, O., Hashimoto, T. and Lior, N., 1993, The relationship between flow pattern and thermal non-equilibrium in the multi-stage flash evaporation process. *Desalination* **91**, 51–64.
- Miyatake, O., Tomimura, T. and Ide, Y., 1985, Enhancement of spray flash evaporation by means of the injection of bubble nuclei. *ASME J. Solar Energy Engng* **107**, 176–182.
- Moalem-Maron, D. and Zijl, W., 1978, Growth, condensation and departure of small and large vapour bubbles in pure and binary systems. *Chem. Engng Sci.* **11**, 1339–1346.
- NRC (National Research Council of the U.S.A.), 1927, *International Critical Tables*, II, p. 328. McGraw-Hill, New York.
- NRC (National Research Council of the U.S.A.), 1928a, *International Critical Tables*, III, p. 369. McGraw-Hill, New York.
- NRC (National Research Council of the U.S.A.), 1928b,

- International Critical Tables*, IV, p. 465. McGraw-Hill, New York.
- NRC (National Research Council of the U.S.A.), 1929, *International Critical Tables*, V, pp. 15, 67, 115. McGraw-Hill, New York.
- Olson, R. L. and Walton, J. S., 1951, Diffusion coefficients of organic liquids in solution. *Ind. Engng Chem.* **43**, 703–706.
- ORNL (Oak Ridge National Laboratory), 1966, *The Oak Ridge National Laboratory Conceptual Design of a 250-MGD Desalination Plant*. U.S. Department of the Interior, Office of Saline Water R&D Progress Report No. 214, p. 226.
- Ozbek, H. and Phillips, S. L., 1980, Thermal conductivity of aqueous NaCl solutions from 20 to 330°C. *J. chem. Engng Data* **25**, 263–267.
- Pinto, Y. and Davis, E. J., 1971, The motion of vapor bubbles growing in uniformly superheated liquids. *A.I.Ch.E. J.* **17**, 1452–1458.
- Plesset, M. S. and Prosperetti, A., 1977, Bubble dynamics and cavitation. *Ann. Rev. Fluid Mech.* 145–185.
- Plesset, M. S. and Zwick, S. A., 1952, A nonsteady heat diffusion problem with spherical symmetry. *J. appl. Phys.* **23**, 95–98.
- Plesset, M. S. and Zwick, S. A., 1954, The growth of vapor bubbles in superheated liquids. *J. appl. Phys.* **25**, 493–500.
- Prosperetti, A., 1982, Bubble dynamics: a review and some recent results. *Appl. Sci. Res.* **38**, 145–164.
- Prosperetti, A. and Plesset, M. S., 1978, Vapor-bubble growth in a superheated liquid. *J. Fluid Mech.* **85**, 349–368.
- Saito, T. and Shima, A., 1977, Numerical solution for the spherical bubble growth problem in a uniformly ultra-heated liquid. *J. Mech. Engng Sci.* **19**, 101–107.
- Sato, K., 1974, Simplified expressions for state quantities of saturated water and steam. *Bull. Soc. Sea Water Sci. Japan* **28**, 182–190.
- Scriven, L. E., 1959, On the dynamics of phase growth. *Chem. Engng Sci.* **10**, 1–13.
- Skinner, L. A. and Bankoff, S. G., 1964, Dynamics of vapour bubbles in binary liquids with spherically symmetric initial conditions. *Phys. Fluids* **7**, 643–648.
- Stokes, R. H., 1950, The diffusion coefficients of eight uni-valent electrolytes in aqueous solution at 25°C. *J. Am. chem. Soc.* **72**, 2243–2247.
- Theofanous, T. G. and Patel, P. D., 1976, Universal relations for bubble growth. *Int. J. Heat Mass Transfer* **19**, 425–429.
- van Stralen, S. J. D., 1968, The growth rate of vapour bubbles in superheated pure liquids and binary mixtures—Parts I and II. *Int. J. Heat Mass Transfer* **11**, 1467–1490, 1491–1512.
- van Strale, S. J. D. and Zijl, W., 1978, Fundamental developments in bubble dynamics, in *Proceedings of the 6th International Heat Transfer Conference*, Toronto, Canada, Vol. 6, pp. 429–449. Hemisphere, New York.
- Yatabe, J. M. and Westwater, J. W., 1966, Bubble growth rates for ethanol-water and ethanol-isopropanol mixtures. *Chem. Engng Prog. Symp. Ser.* **64**, **62**, 17–23.
- Yusufova, V. D., Pepinov, R. I., Nicolayev, V. A., Zokhr, G. U., Lobcova, N. V. and Tuayev, 1978, Thermophysical properties of softened salt solutions over a wide temperature range. *Desalination* **25**, 269–280.